Self-generation of chaotic dissipative multisoliton complexes supported by competing nonlinear spin-wave interactions

Sergey V. Grishin,[1,*] Boris S. Dmitriev,[2] Olga I. Moskalenko,[3] Valentin N. Skorokhodov,[1] and Yurii P. Sharaevskii[2]
[1]*Department of Electronics, Oscillations and Waves, Saratov State University, Saratov 410012, Russia*
[2]*Department of Nonlinear Physics, Saratov State University, Saratov 410012, Russia*
[3]*Department of Open System Physics, Saratov State University, Saratov 410012, Russia*

(Received 13 November 2017; revised manuscript received 8 June 2018; published 13 August 2018)

A self-generation of chaotic dissipative spin-wave multisoliton complexes has been observed experimentally. Localized in time, these patterns are formed in a passively Q-switched and mode-locked magnetic film feedback ring due to the competing three- and four-wave nonlinear spin-wave interactions. Such competition induces a modulation instability that leads to the formation of incoherent one-color four-wave bound solitons embedded in chaotic three-wave solitonlike pulses. The development of a symmetry-breaking instability causes a transition from incoherent one-color four-wave bound solitons to chaotic multicolor ones.

DOI: 10.1103/PhysRevE.98.022209

Dissipative solitons are one of the modern paradigms of nonlinear dynamics and the theory of self-organization. Unlike conservative solitons, dissipative solitons in photonics are formed due to the competition between gain and loss as well as between dispersion or diffraction and nonlinearity [1–3]. Unlike single dissipative solitons, complex soliton structures composed of several interacting dissipative solitons have been observed in optical systems [1–3], Bose-Einstein condensates [4,5], and magnetic film feedback rings (MFFRs) [6–8].

In nonlinear optics, multisoliton complexes [9–13] and soliton clusters [14–16] consisting of temporal, spatial, or spatiotemporal interacting (bound) solitons have been explored. The multisoliton complexes of temporal bound solitons are formed both in optical fiber [9–11] and in passively mode-locked fiber laser rings with dispersion management [12,13]. The soliton clusters contain either two-dimensional spatial solitons [14,15] or three-dimensional light bullets [16] that are self-localized due to competing quadratic and cubic nonlinearities. The competing nonlinearities provide also the stability of bound states to the random perturbations. Both the periodic change of group velocity dispersion from positive to negative and the competition between self-focusing and self-defocusing nonlinearities cause the stable formation of a two-color soliton [9,14]. Such a bound state, known as a "soliton molecule," consists of two antiphase bright solitons coupled together by a dark soliton [9]. The soliton molecule has properties similar to those of a diatomic molecule of matter, and it can be used as a stable upper bit in optical communications [13].

Among two-dimensional soliton clusters, there are ringlike solitons propagating in saturable self-focusing media [17,18]. The relative phase between two neighboring solitons of such a cluster is calculated by the following expression [17]:

$$\theta = 2\pi m/N, \tag{1}$$

where N is the number of solitons and m determines the full phase twist around the ring. During propagation, the ringlike solitons are rotated and able to disintegrate into a set of isolated two-dimensional spatial solitons due to symmetry-breaking instability [19,20].

For the MFFRs, a number of experimental results have been obtained for self-generation of single bright or dark spin wave envelope solitons [6,21–23]. The periodic and chaotic trains of such pulses are formed either due to four-wave [6] or three-wave [21–23] nonlinear interactions. There are only a few works describing spin-wave multisoliton generation [7,8]. In those works, the multisolitons are excited by stationary magnetic pumping. The variation of the repetition rate of pumping pulses causes the half-frequency generation of multisolitons that consist of two or three one-color backward volume spin-wave solitons. In both cases, the symmetry-breaking soliton modes have a relative phase equal to π [7].

In the above-mentioned works, spin-wave multisolitons were generated when the chaotic mode was absent in a ring. However, such a mode can be achieved in an autonomous MFFR in which a magnetostatic spin wave (MSW) plays the role of nonstationary pumping. It is well known that at certain frequency and power conditions, the MSW can take part both in three-wave decay processes and in four-wave nonlinear spin-wave interactions [24,25]. The simultaneous presence of both nonlinear interactions leads to the self-generation of a wide-band chaotic signal that consists of solitary chaotic pulses [26]. But, such pulses are not the bound solitons.

Following the optical systems [13], a passively mode-locked MFFR with MSW pumping can be regarded as a good candidate for generation of multisoliton complexes. In this paper, we report on the chaotic multisoliton complex generation in such a system that supports the competition between three- and four-wave interactions.

The explored MFFR consists of both vacuum and solid-state linear and nonlinear elements (see Fig. 1). Two drift klystron amplifiers and one solid-state preamplifier operating in a linear regime of amplification are used for both the ring eigenmode

*grishfam@sgu.ru

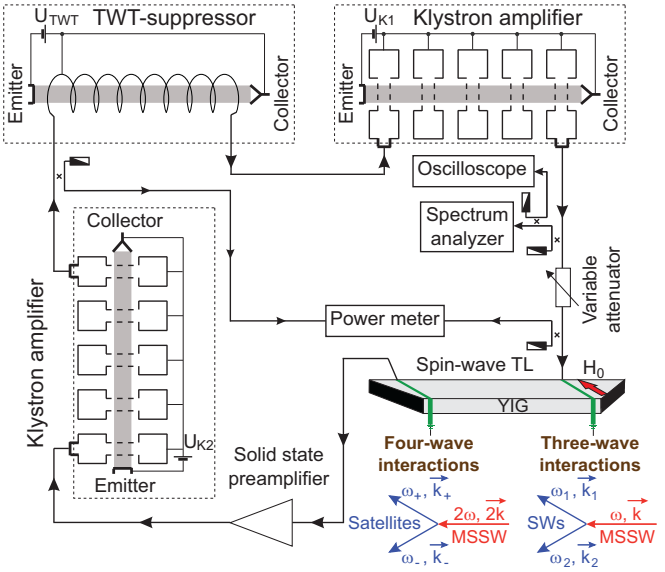

FIG. 1. Schematic diagram of MFFR that supports the competition between three- and four-wave interactions.

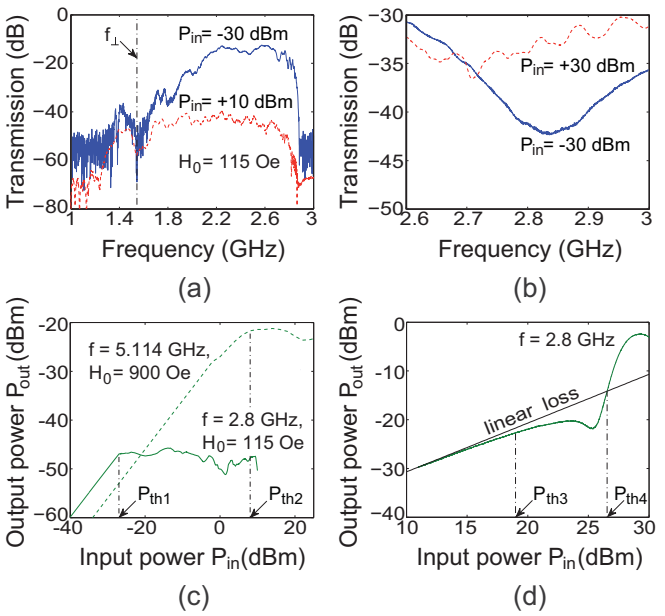

FIG. 2. (a),(b) Transmission characteristics and (c),(d) power responses of (a),(c) the spin-wave TL and (b),(d) the TWT suppressor. In (a), a frequency of $f_\perp = \sqrt{f_H(f_H + f_M)}$ (where $f_H = \gamma H_{\text{int}}$, $H_{\text{int}} = H_0 + H_a + H_d$, $f_M = 4\pi\gamma M_0$, and $\gamma = 2.8$ MHz/Oe) is a MSSW cutoff frequency. All TWT responses are measured at an accelerating voltage of $U_{\text{TWT}} = 1980$ V and a beam current of $I_{\text{TWT}} = 17.3$ mA.

selection and the ring loss compensation. A spin-wave transmission line (TL) and a traveling-wave tube (TWT) suppressor are used for Q-switching and mode-locking techniques. A signal power level in the feedback loop is adjusted by means of a variable attenuator and controlled at the spin-wave TL and the TWT-suppressor inputs by a two-channel power meter. A produced signal is fed to the inputs of a spectrum analyzer and a real-time oscilloscope for the following processing.

The spin-wave TL contains the input and output microstrip transducers located at a distance of 7 mm from each other. A yttrium-iron-garnet (YIG) film with a saturation magnetization of $4\pi M_0 = 1750$ Gs is placed on top of both transducers. It has a thickness of 65 μm, a width of 4 mm, and a length of 10 mm. The input transducer excites the MSWs in the YIG film, and the output transducer detects them. An external bias magnetic field $H_0 = 115$ Oe is applied to a YIG film surface and directed along both transducers. In this case, a magnetostatic surface spin wave (MSSW) is excited at the frequencies where both three-wave and four-wave nonlinear spin-wave interactions are allowed [24,25].

The spiral-type TWT operates as a signal suppressor in the Kompfner deep mode [27]. In this mode, a gyro-TWT-suppressor was used as a fast saturable absorber in a gyro-TWT generator model for passive mode-locking and self-generation of ultrashort pulses [28]. It is necessary to note that in a microwave region, a MSW signal-to-noise enhancer also has responses corresponding to a saturable absorber [29]. However, in all previous works [30,31] the MSW suppressor was used as a slow saturable absorber in a feedback loop of a ferromagnetic film active ring resonator, because the relaxation time of the MSW suppressor was much greater than that of a ring's round-trip time. In these works, multimode generation through four-wave interactions was not achieved, and a giant pulse self-generation was obtained only through three-wave interactions.

As shown in Figs. 2(a) and 2(b), the two above-mentioned nonlinear elements have opposite dependencies to transmission loss on input power. For the spin-wave TL, the transmission loss is increased with the growth of the input power, but for the TWT suppressor the transmission loss is decreased. The transmission loss of the spin-wave TL grows due to three- and four-wave interactions. To determine the power thresholds corresponding to both interactions, the output power versus input power responses were measured at two values of H_0. Both power measurements were carried out at frequencies at which a MSSW wave number has the same value of $k = 195$ cm^{-1}. As follows from Fig. 2(c), three-wave power threshold measured at $H_0 = 115$ Oe ($H_a = 52$ Oe is an anisotropy field and $H_d = -12$ Oe is a demagnetized field) has a value of $P_{\text{th1}} = -27$ dB m. At the same time, the four-wave power threshold measured at $H_0 = 900$ Oe ($H_a = 80$ Oe and $H_d = -12$ Oe), where three-wave interactions are forbidden [24,25], has a value of $P_{\text{th2}} = +8$ dB m. Both power thresholds have strongly different values and $P_{\text{th2}} \gg P_{\text{th1}}$. Thus, in all amplitude responses measured at $H_0 = 115$ Oe, four-wave interactions definitely exist at $P_{\text{in}} \geqslant P_{\text{th2}}$.

The TWT-suppressor power response has two thresholds of $P_{\text{th3}} = +19$ dB m and $P_{\text{th4}} = +26.5$ dB m. If the input power values lie in a range of $P_{\text{th3}} < P_{\text{in}} < P_{\text{th4}}$, then the output power is limited because electrons drift in the region of accelerating phases of an electromagnetic field. If $P_{\text{in}} > P_{\text{th4}}$, then the output power is increased and it exceeds a linear loss level. In this case, electrons drift in the region of decelerating phases of the field, and the TWT operates as a saturable absorber.

For the MFFR, both passive Q-switching and mode-locking techniques are realized if signal power levels at the inputs of spin-wave TL and TWT suppressor are greater than the thresholds of P_{th2} and P_{th4}, respectively. The experimental

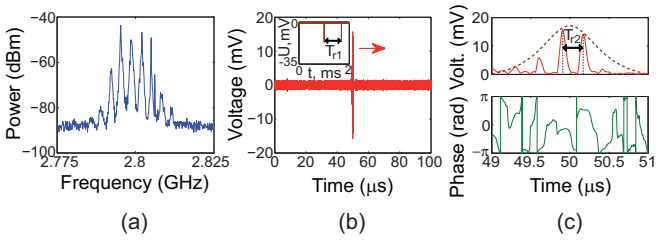

FIG. 3. (a) Power-frequency spectrum and (b),(c) time series of one-color multisoliton complexes self-generated at $G = 0$. The pulses presented in the inset of (b) were measured by the envelope detection method. The amplitude [(a), top panel] and phase [(a), bottom panel] profiles in (c) were obtained by applying a Hilbert transform to the microwave time series [23].

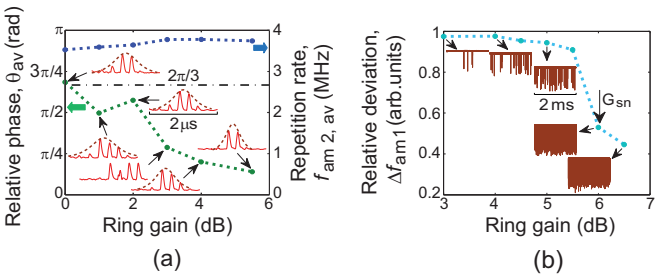

FIG. 4. Dependencies of (a) averaged relative phase and repetition rate of four-wave solitons, and (b) relative deviation of the repetition rate of three-wave solitonlike pulses on the ring gain.

results satisfying both power conditions are presented in the following figures.

As shown in Fig. 3, at a ring gain $G = 0$ (where $G = K - A$, K is the total amplification, and A is the total loss in the ring), a chaotic train of dissipative multisoliton complexes is rigidly self-generated. The multisoliton complexes consist of both three- and four-wave dissipative solitons that are generated through various physical mechanisms. So, three-wave solitonlike pulses are formed due to Q-switching of the ring resonator by parametrically excited spin waves [23]. These pulses have a large width of $T_{d1} \simeq 1$ μs, which depends on the relaxation time of spin waves (SWs). The phase mismatch between parametrically bound MSW and SWs produces parametric three-wave turbulence [24,32] that causes the chaotic variation of a repetition rate of $f_{\mathrm{am1}} = 1/T_{r1}$ and leads to chaotization of each ring eigenmode spectrum [see Fig. 3(a)]. As follows from the inset in Fig. 3(b), the frequencies of f_{am1} of all ring eigenmodes have a minimum value of about 1.4 kHz. Three-wave solitonlike pulses are formed during many cycles of a signal around the ring ($T_{d1} \gg \tau_{\mathrm{rg}}$, where $\tau_{\mathrm{rg}} \simeq 300$ ns is a ring round trip time) and they are analogs of optical temporal solitons [23]. The amplitude profile of such pulses is well approximated by the hyperbolic secant function [see the dashed line in Fig. 3(c)]. Their peak power of $P_p = +16$ dB m, measured at the input of spin-wave TL, is much greater than the peak power of three-wave pulses that are self-generated when the TWT suppressor is absent in the ring. Thus, three-wave solitonlike pulses are giant amplitude pulses.

Four-wave dissipative solitons are self-generated through the modulation instability produced by the competition between three- and four-wave nonlinear spin-wave interactions [33]. Unlike parametric solitonlike pulses, four-wave solitons are formed during one cycle of a signal around the ring, because $T_{d2} \ll \tau_{\mathrm{rg}}$ (where $T_{d2} \simeq 80$ ns is the width of a four-wave soliton). As shown in an enlarged fragment of the time series [see Fig. 3(c), top panel], three four-wave solitons are embedded in a single three-wave solitonlike pulse. The peak amplitudes of four-wave solitons are unstable from one giant pulse to another, because the amplitude profiles of giant pulses are formed under parametric turbulence. At the same time, the temporal separation between four-wave solitons is practically stationary, which leads to a constant coupling between four-wave solitons located inside each giant pulse. The separation corresponds to the frequency interval Δf between the neighboring eigenmodes [see Fig. 3(a)] involved in the process of passive mode-locking. The averaged value of a self-modulation frequency $f_{\mathrm{am2,av}} = 1/T_{r2,\mathrm{av}} \simeq 3.6$ MHz practically coincides with the averaged value of $\Delta f_{\mathrm{av}} \simeq 3.2$ MHz and sets a repetition rate of four-wave solitons. The amplitude of such pulses is also well approximated by the hyperbolic secant function, but their phase is not flat and it has a clear chirp inside each pulse. As a result, these nonlinear pulses do not correspond to the conservative solitons [34] and they are regarded as dissipative chirped solitons [2]. The relative phase between two neighboring four-wave solitons has a value of about $2\pi/3$ [see Fig. 3(c), bottom panel], which corresponds to the analogous value calculated from the expression (1) for $N = 3$ and $m = 1$. This fact indicates that four-wave solitons are bound solitons. However, for optical ringlike solitons it has been shown that three coherently interacting solitons cannot form a bound state, and that it can be formed only due to incoherent interaction [17]. In our case, parametric turbulence influences the relative phase, which results in its slight difference from $2\pi/3$. This leads to incoherent interaction of four-wave solitons and the formation of incoherent bound states.

As follows from Fig. 4, the multisoliton complexes consisting of one-color (bright) bound solitons are observed when the ring gain is increased from 0 to 5.5 dB. In this case, the averaged frequency of $f_{\mathrm{am2,av}}$ is increased, which leads to the growth of coupling between soliton modes [see Fig. 4(a)]. However, the coupling does not achieve a value corresponding to the soliton mode chaotization. This is confirmed by the temporal response of the frequencies f_{am2} that have insignificant fluctuations at $G = 4$ dB [see Fig. 5(a)]. The growth of G leads also to the variation of the relative phase between soliton modes [see Fig. 4(a)] that is smoothly decreased by the value of about 100°. At $G = 5.5$ dB, the relative phase has a minimal value and the phase symmetry tends to be restored. In the previous work [7], the relative phase has a value equal to π corresponding to one symmetry-breaking mode. In our case, all soliton modes have symmetry-breaking of phase periodicity. Moreover, with the growth of G there is a competition between the number of soliton modes that take part in the formation of one-color bound states. They consist of two ($G = 5.5$ dB), three ($G = 0$), or even four ($G = 3$ dB) bound four-wave solitons. The ring gain also influences the characteristics of three-wave solitonlike pulses. As follows from the insets in Fig. 4(b), the repetition rate of such pulses is increased with the

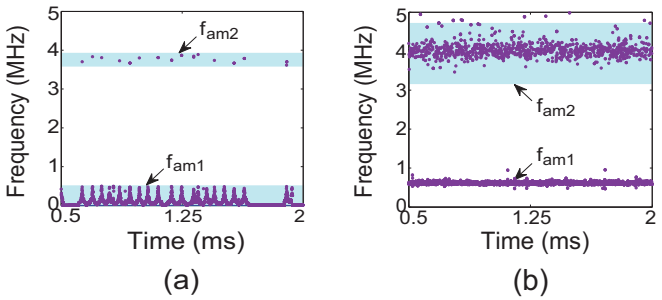

FIG. 5. Temporal variations of repetition rates f_{am1} and f_{am2} obtained at two values of the ring gain: (a) $G = 4$ dB and (b) $G = 6.5$ dB. The frequencies have been obtained by means of continuous wavelet transform with complex basis [35].

growth of G. It causes the spectra expansion of all eigenmodes and their partial overlap. In the time domain [see Fig. 5(a)], the frequencies of f_{am1} of all eigenmodes fluctuate from 5 to 500 kHz, and in contrast to the frequencies of f_{am2}, they are not synchronized.

For the explored dynamical system, the ring gain value of $G = 6$ dB is a bifurcation point. At this point, the incoherent one-color multisoliton complexes are transformed into chaotic multicolor ones through symmetry-breaking instability. In Fig. 6, there are experimental results of self-generation of multicolor multisoliton complexes that are measured when the ring gain slightly exceeds the bifurcation value. As follows from Fig. 6(a), the spectra of all ring eigenmodes are completely overlapped. This leads to desynchronization of the frequencies f_{am2} and chaotic synchronization of the frequencies f_{am1} that have practically stationary values of $f_{am1} \simeq 600$ kHz [see Fig. 5(b)]. The ring gain threshold of G_{sn} corresponding to the

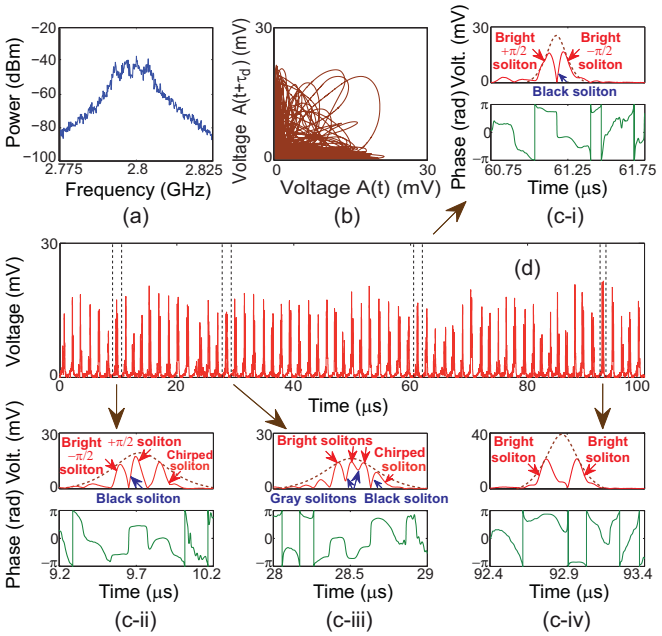

FIG. 6. (a) Power-frequency spectrum, (b) phase portrait, [(c), top panels, and (d)] amplitude, and [(c), bottom panels] phase profiles of multicolor multisoliton complexes self-generated at $G = 6.5$ dB.

synchronization regime of frequencies f_{am1} is clearly visible in Fig. 4(b). At this threshold, the relative value of deviation of self-modulation frequencies of parametrically excited SWs of $\Delta f_{am1} = (f_{am1}^{max} - f_{am1}^{min})/f_{am1}^{max}$ (where f_{am1}^{max} is a maximal value of f_{am1} and f_{am1}^{min} is its minimal value) is abruptly decreased more than twice.

As follows from Figs. 6(c) and 6(d), the multicolor multisoliton complexes consist of two (c-i, c-iv), three (c-ii), and four (c-iii) bound four-wave solitons. Unlike one-color multisoliton complexes, bright solitons contained in multicolor ones are coupled together by dark (black or gray) solitons. It is well known [6] that for a black soliton, an amplitude at a dip goes completely to zero, and a phase inside the dip has a jump equal exactly to π. For a gray soliton, the amplitude at the dip is not equal to zero and the jump in phase is less than π.

In Figs. 6(c-i), there is a bound state of two antiphase bright solitons that are coupled together by the black soliton. Both bright solitons have a flat phase inside each pulse, and the black soliton has a clear jump in phase equal to π. Such a bound state corresponds to the temporal soliton molecule [9] that is observed in the microwave region. The chaotization of f_{am2} causes the chaotic variation of coupling between two bright solitons. As follows from Fig. 6(c-iv), the separation between two bright solitons can achieve a value at which the black soliton disappears. At the same time, the symmetry-breaking instability leads to the appearance of more complicated bound states. In Fig. 6(c-ii), there is a bound state that consists of one chirped soliton and two bright solitons possessing unequal amplitudes. Two bright solitons are coupled together by the black soliton. However, the separation between bright and chirped solitons is great enough to form a second black soliton. In Fig. 6(c-iii), three bright solitons are coupled with one chirped soliton by the black soliton. The coupling between these bright solitons is realized through the gray solitons. All of the multicolor multisoliton complexes described above are nonstationary because they are formed in the regime of four-wave dynamical chaos. The phase portrait of such bound states is typical for the dynamical chaos possessing a large dimension [see Fig. 6(b)].

In summary, in this paper we reported an experimental observation of chaotic multisoliton complexes self-generated in a dissipative microwave system with gain and loss as well as with competing three- and four-wave interactions. One of the main features of our research is the formation of one-dimensional bound solitons under the influence of spin-wave turbulence. The presence of only three-wave turbulence leads to the creation of the relatively simple (one-color) chaotic bound solitons. At the same time, the development of turbulence through three- and four-wave nonlinear interactions gives us a chance to create more complex states in the form of multicolor chaotic bound solitons. The obtained results may be of interest to researchers exploring complex pattern formation in various fields of science.

The work was supported by the Russian Foundation for Basic Research (Project No. 18-02-00666). We would like to thank Dmitrii I. Trubetskov for useful discussions and Maksim Zhuravlev for help with the numerical calculations of the wavelet spectrum energies.

[1] N. Rosanov, *Spatial Hysteresis and Optical Patterns* (Springer, Berlin, 2002).

[2] N. N. Akhmediev and A. Ankiewicz, *Dissipative Solitons* (Springer-Verlag, Berlin, 2005).

[3] P. Grelu, *Nonlinear Optical Cavity Dynamics* (Wiley-VCH, Weinheim, 2016).

[4] C. J. Pethick and H. Smith, *Bose-Einstein Condensation in Dilute Gases* (Cambridge University Press, Cambridge, 2002).

[5] K. Lakomy, R. Nath, and L. Santos, Phys. Rev. A **86**, 013610 (2012).

[6] M. Wu, Solid State Phys. **62**, 163 (2010).

[7] S. O. Demokritov, A. A. Serga, V. E. Demidov *et al.*, Nature (London) **426**, 159 (2003).

[8] A. A. Serga, M. P. Kostylev, B. A. Kalinikos *et al.*, JETP **102**, 497 (2006).

[9] M. Stratmann, T. Pagel, and F. Mitschke, Phys. Rev. Lett. **95**, 143902 (2005).

[10] P. Rohrmann, A. Hause, and F. Mitschke, Sci. Rep. **2**, 866 (2012).

[11] K. Krupa, K. Nithyanandan, U. Andral, P. Tchofo-Dinda, and P. Grelu, Phys. Rev. Lett. **118**, 243901 (2017).

[12] A. Haboucha, H. Leblond, M. Salhi, A. Komarov, and F. Sanchez, Phys. Rev. A **78**, 043806 (2008).

[13] P. Grelu and N. Akhmediev, Nat. Photon. **6**, 84 (2012).

[14] Y. V. Kartashov, L. C. Crasovan, D. Mihalache, and L. Torner, Phys. Rev. Lett. **89**, 273902 (2002).

[15] A. Fratalocchi, A. Piccardi, M. Peccianti, and G. Assanto, Phys. Rev. A **75**, 063835 (2007).

[16] L.-C. Crasovan, Y. V. Kartashov, D. Mihalache, L. Torner, Y. S. Kivshar, and V. M. Pérez-Garcia, Phys. Rev. E **67**, 046610 (2003).

[17] A. S. Desyatnikov and Y. S. Kivshar, Phys. Rev. Lett. **88**, 053901 (2002).

[18] A. S. Desyatnikov and Y. S. Kivshar, J. Opt. B **4**, S58 (2002).

[19] V. Tikhonenko, J. Christou, and B. Luther-Davies, Phys. Rev. Lett. **76**, 2698 (1996).

[20] D. V. Petrov, L. Torner, J. Martorell, R. Vilaseca, J. P. Torres, and C. Cojocaru, Opt. Lett. **23**, 1444 (1998).

[21] E. N. Beginin, S. V. Grishin, and Y. P. Sharaevsky, JETP Lett. **88**, 647 (2008).

[22] S. V. Grishin, E. N. Beginin, Y. P. Sharaevskii, and S. A. Nikitov, Appl. Phys. Lett. **103**, 022408 (2013).

[23] S. V. Grishin, T. M. Golova, M. A. Morozova *et al.*, JETP **121**, 623 (2015).

[24] V. S. L'vov, *Wave Turbulence Under Parametric Excitation* (Springer-Verlag, Berlin, 1994).

[25] A. G. Gurevich and G. A. Melkov, *Magnetization Oscillations and Waves* (CRC, New York, 1996).

[26] M. Wu, B. A. Kalinikos, and C. E. Patton, Phys. Rev. Lett. **95**, 237202 (2005).

[27] R. Kompfner, J. Brit. IRE **10**, 283 (1950).

[28] N. S. Ginzburg, G. G. Denisov, Vilkov *et al.*, Phys. Plasmas **24**, 023103 (2017).

[29] J. D. Adam and S. N. Stitzer, Appl. Phys. Lett. **36**, 485 (1980).

[30] E. N. Beginin, S. V. Grishin, and Y. P. Sharaevsky, Tech. Phys. Lett. **36**, 1042 (2010).

[31] S. V. Grishin, B. S. Dmitriev, S. A. Nikitov *et al.*, IEEE Trans. Magn. **48**, 4382 (2012).

[32] V. E. Demidov and N. B. Kovshikov, Tech. Phys. **44**, 960 (1999).

[33] M. A. Cherkasskii, N. G. Kovshikov, and B. A. Kalinikos, Phys. Solid State **52**, 2123 (2010).

[34] J. M. Nash, P. Kabos, R. Staudinger, and C. E. Patton, J. Appl. Phys. **83**, 2689 (1998).

[35] A. E. Hramov, A. A. Koronovskii, O. I. Moskalenko, M. O. Zhuravlev, R. Jaimes-Reategui, and A. N. Pisarchik, Phys. Rev. E **93**, 052218 (2016).